Time Domain Multiplexed LoRa Modulation Waveform Design for IoT Communication

Shixiang An, Hua Wang, *Member, IEEE*, Yiwei Sun, Zhiping Lu, and Quantao Yu

***Abstract*— Long-Range (LoRa) is one of the emerging technologies in low-power wide-area networks (LPWANs). In this letter, we proposed a Time Domain Multiplexed LoRa (TDM-LoRa) modulation to improve the throughput of conventional LoRa by using up-chirp and down-chirp simultaneously. A low complexity non-coherent algorithm for the TDM-LoRa modulation is also presented. We then derive an analytical expression for the bit error rate (BER) of non-coherent demodulation in the additive white Gaussian noise (AWGN) channel. In addition, a scheme that encodes information bits on both in-phase and quadrature components of the TDM-LoRa symbol is presented to further improve the system data rate. Performance analysis and simulation show that our proposed schemes can achieve better spectral efficiency (SE) and throughput without obvious bit error rate (BER) degradation compared to the LoRa Physical Layer (PHY) scheme.**

***Index Terms*— LPWANs, LoRa, TDM-LoRa, IoT.**

I. Introduction

THE development of Internet of Things (IoT) is an extremely challenging topic, and the debate on how to put it into practice is still open. IoT allows a massive deployment of sensors to collect and process all sorts of data, thus creating opportunities for a vast range of new applications. Low-Power Wide-Area Networks (LPWANs) are key enablers for the emerging IoT technology [1], [2].

LoRa is a new LPWAN PHY solution, designed and patented by Semtech Corporation [2]. The LoRa modulation is often referred to "chirp modulation". The information-bearing element is the frequency shift and the chirp is similar to a carrier [3]. Spreading factor (SF) and the bandwidth (B) are the most important parameters in LoRa modulation. Increasing SF can significantly extend the communication range, but it comes at the cost of transmission rate. Although providing flexibility in the data rate, the achievable rate of LoRa modulation still limits many applications.

Researchers have proposed different modifications for the conventional LoRa modulation to improve its maximum achievable data rate [4]–[8]. References [4] and [5] are proposed to encode extra information bits on the phase of the chirp waveform. Although these methods improve the achievable data rate, the receivers need highly accurate channel state information. The increased complexity of receivers not only increases cost but also reduces battery life. Interleaved Chirp Spreading LoRa (ICS-LoRa) has been introduced as a new multidimensional space generated from interleaved versions of the nominal LoRa network in [6]. Although the interleaved chirps in ICS-LoRa modulation keep a constant envelope, they suffer from a rather high correlation with the basic up-chirp, causing BER degradation of ICS-LoRa modulation. Reference [7] implements down-chirp and its cyclic shifts instead of interleaved chirps used in ICS-LoRa modulation. The proposed scheme known as slope-shift keying (SSK) outperforms the ICS-LoRa modulation scheme without incurring additional complexity. However, the SSK-LoRa only have one bit data rate increase during a symbol time. The scheme, called as in-phase and quadrature chirp spread spectrum (IQCSS) proposed in [8], doubles the date rate and SE when compared to the conventional LoRa PHY scheme. IQCSS encodes information bits on both in-phase and quadrature components of the chirp signal. Hence, channel equalization and strict synchronization are required for compensating the channel-induced phase rotation on the transmit signal. An interesting aspect of IQCSS is that the receiver is still able to decode the information transmitted using the original LoRa modulation.

In this letter, we propose a new TDM-LoRa modulation. Furthermore, we present a low complexity non-coherent demodulation algorithm of the proposed TDM-LoRa modulation and obtain an analytical expression for the BER in the AWGN channel. In addition, to further improve the data rate using the proposed waveforms, we introduce IQCSS [8] along with our TDM-LoRa scheme and design the In-phase and Quadrature Time Domain Multiplexed LoRa (IQTDM-LoRa) modulation.

II. Proposed Time Domain Multiplexed LoRa

A. LoRa Modulation

LoRa adopts the Chirp Spread Spectrum (CSS) modulation. LoRa modulation converts data information into chirp symbols. The frequency range and data rate of LoRa modulation depend on the bandwidth B and spreading factors $SF \subset \{6, 7, 8, \ldots 12\}$. The signal frequency varies between $-B/2$ and $B/2$ at baseband. Since LoRa modulation order is defined as $M = 2^{SF}$, each symbol of LoRa modulation can carry SF bits with symbol period $T = 2^{SF}/B$. Thus the SE of LoRa modulation is

$$(SF/T)/B = SF/(B \cdot T) = SF/2^{SF}. \tag{1}$$

A discrete time raw up-chirp sampled at Nyquist sampling rate B, denoted by $s_u(n)$, in its complex baseband-equivalent

Manuscript received December 24, 2021; revised January 18, 2022; accepted January 24, 2022. Date of publication January 26, 2022; date of current version April 11, 2022. This work was supported by the National Key Research and Development Program of China under Grant 2020YFB1807900. The work was also supported by Datang Linktester Technology Co., Ltd. The associate editor coordinating the review of this letter and approving it for publication was Z. Qin. *(Corresponding author: Hua Wang.)*

The authors are with the School of Information and Electronics, Beijing Institute of Technology, Beijing 100081, China (e-mail: wanghua@bit.edu.cn).

Digital Object Identifier 10.1109/LCOMM.2022.3146511

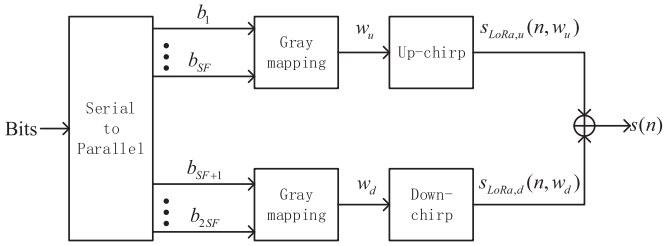

Fig. 1. Transmitter of the proposed TDM-LoRa scheme.

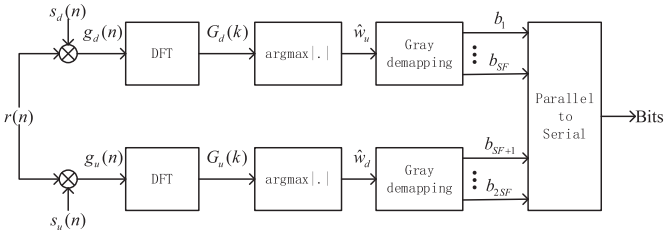

Fig. 2. Receiver of the proposed TDM-LoRa scheme.

form, is given by [7], [8]

$$s_u(n) = 1/\sqrt{M}\exp(j\pi(n^2/M - n)), \tag{2}$$

where $n = 0, 1, 2, \ldots M-1$ depicts the sample index at the time n/B. A complex-baseband discrete time raw down-chirp, denoted by $s_d(n)$, is related to $s_u(n)$ as

$$s_d(n) = s_u^*(n) = 1/\sqrt{M}\exp(j\pi(-n^2/M + n)), \tag{3}$$

In LoRa modulation, which is a frequency-shift chirp modulation, a total of M orthogonal up-chirps are used. $s_u(n)$ and its cyclic shifts are used for representing the information. Every group of SF bits is mapped to $w_u \subset \{1, 2, \ldots M\}$. The normalized discrete time LoRa symbol carrying w_u can be described as

$$s_{LoRa,u}(n, w_u) = 1/\sqrt{M}\exp(j\pi((n^2 + 2w_u n)/M - n)). \tag{4}$$

B. TDM-LoRa Modulation

The core idea of TDM-LoRa is to introduce a down-chirp along with an up-chirp into a TDM-LoRa symbol. Fig. 1 shows the transmitter of the TDM-LoRa modulation. Each TDM-LoRa symbol carries $2SF$ bits, the first SF bits are mapped to w_u, and the last are mapped to w_d. In this way, TDM-LoRa achieves 2 times data rate of LoRa, and its SE is

$$(2SF/T)/B = 2SF/(B \cdot T) = 2SF/2^{SF}. \tag{5}$$

The discrete time down-chirp component carrying w_d can be expressed as:

$$s_{LoRa,d}(n, w_d) = 1/\sqrt{M}\exp(j\pi((-n^2 + 2w_d n)/M + n)), \tag{6}$$

therefore, the normalized TDM-LoRa symbol can be written as:

$$s(n) = (s_{LoRa,u}(n, w_u) + s_{LoRa,d}(n, w_d))/\sqrt{2}. \tag{7}$$

C. Non-Coherent Demodulation

Fig. 2 is the non-coherent demodulation scheme of TDM-LoRa. Assuming perfect synchronization, the received symbol is

$$r(n) = s(n) + w(n), \tag{8}$$

where $w(n)$ is additive white Gaussian noise. To recover w_u, $r(n)$ is multiplied by $s_d(n)$ to de-chirp the up-chirp component. We can get $g_d(n)$ as follows:

$$\begin{aligned} g_d(n) &= r(n)s_d(n) \\ &= s(n)s_d(n) + w(n)s_d(n) \\ &= (g_{u,d}(n) + g_{d,d}(n))/\sqrt{2} + w(n)s_d(n), \end{aligned} \tag{9}$$

where

$$\begin{aligned} g_{u,d}(n) &= s_{LoRa,u}(n, w_u)s_d(n) \\ &= 1/M\exp(j\pi((2w_u n)/M)), \end{aligned} \tag{10}$$

and

$$\begin{aligned} g_{d,d}(n) &= s_{LoRa,d}(n, w_d)s_d(n) \\ &= 1/M\exp(j\pi((-2n^2 + 2w_d n)/M + 2n)). \end{aligned} \tag{11}$$

Symbol demodulation can be done by performing M-point DFT on the de-chirped signal $g_d(n)$, then we have

$$\begin{aligned} G_d(k) &= |DFT[r(n)s_d(n)]| \\ &= |\sum_{n=0}^{M-1} r(n)s_d(n)\exp(-j2\pi nk/M)| \\ &= |\sqrt{\frac{1}{2}}DFT(g_{u,d}(n)) + \sqrt{\frac{1}{2}}DFT(g_{d,d}(n)) \\ &\quad + DFT(w(n)s_d(n))| \\ &= |\sqrt{\frac{1}{2}}G_{u,d}(k) + \sqrt{\frac{1}{2}}G_{d,d}(k) + W(k)| \end{aligned} \tag{12}$$

where

$$\begin{aligned} |G_{u,d}(k)| &= |DFT(g_{u,d}(n))| \\ &= |DFT[s_{LoRa,u}(n, w_u)s_d(n)]| \\ &= |\sum_{n=0}^{M-1} s_{LoRa,u}(n, w_u)s_d(n)e^{-j2\pi kn/M}| \\ &= \delta(w_u - k) \\ &= \begin{cases} 1 & k = w_u \\ 0 & k \neq w_u, \end{cases} \end{aligned} \tag{13}$$

and

$$\begin{aligned} |G_{d,d}(k)| &= |DFT(g_{d,d}(n))| \\ &= |DFT[s_{LoRa,d}(n, w_d)s_d(n)]| \\ &= |\sum_{n=0}^{M-1} s_{LoRa,d}(n, w_d)s_d(n)e^{-j2\pi kn/M}| \\ &= |\sum_{n=0}^{M-1} s_d^2(n)\exp(-j2\pi n(k - w_d)/M)| \\ &= \begin{cases} 0 & (k - w_d)\ is\ even \\ \sqrt{2/M} & (k - w_d)\ is\ odd. \end{cases} \end{aligned} \tag{14}$$

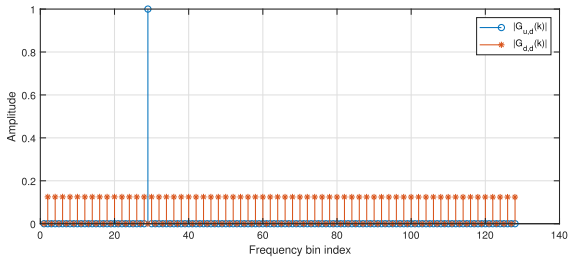

Fig. 3. Envelope of $G_{u,d}(k)$ and $G_{d,d}(k)$.

The DFT operation can be easily carried out via fast Fourier transform (FFT). Fig. 3 illustrates the envelope of $G_{u,d}(k)$ and $G_{d,d}(k)$. According to (11), $g_{d,d}(n)$ is a sweep-frequency signal, the energy of $g_{d,d}(n)$ disperses in frequency domain. While the energy of $g_{u,d}(n)$ concentrates on $f_u = w_u B/2^{SF}$. Therefore, $G_d(k)$ peaks at the w_u^{th} frequency bin index. Then the estimated first SF bits can be obtained according to w_u. Similarly, we can multiply $r(n)$ by $s_u(n)$, and search for the frequency bin index with maximum value from the output of DFT operation to recover w_d and get the last SF bits.

D. Performance Analysis

Notably, the BER performance of TDM-LoRa depends on the original LoRa. Therefore, we first analyze the symbol error rate (SER) performance of LoRa. Let us assume transmission of a LoRa symbol $s_{LoRa,u}(n, w_u)$ over an AWGN channel. The received symbol can be expressed as:

$$r_{LoRa}(n) = s_{LoRa,u}(n, w_u) + w(n), \tag{15}$$

then symbol demodulation can be done by performing M-point DFT on the de-chirped signal to obtain

$$\begin{aligned} G_{LoRa}(k) &= |DFT[r_{LoRa}(n)s_d(n)]| \\ &= |\sum_{n=0}^{M-1} r_{LoRa}(n)s_d(n)\exp(-j2\pi nk/M)| \\ &= |\sum_{n=0}^{M-1} s_{LoRa,u}(n, w_u)s_d(n)\exp(-j2\pi nk/M) \\ &\quad + \sum_{n=0}^{M-1} w(n)s_d(n)\exp(-j2\pi nk/M)| \\ &= |G_{u,d}(k) + W(k)| \\ &= \begin{cases} |1 + W(w_u)| & k = w_u \\ |W(k)| & k \neq w_u, \end{cases} \end{aligned} \tag{16}$$

where $W(k)$ depicts a complex Gaussian noise. Let us define $\zeta(k) = |W(k)|$, $\zeta(k)$ is a Rayleigh distributed random variable with the probability density function (PDF)

$$p_{\mathrm{n}}(\zeta) = (\zeta/\sigma^2)\exp(-\zeta^2/2\sigma^2) \qquad \zeta \geq 0, \tag{17}$$

where $\sigma^2 = N_0/2$ and N_0 is the single-sided noise power spectral density of $W(k)$. We define P_e as the probability SER. P_e can be expressed as

$$P_e = \Pr[\max_{k,k\neq w_u}(\zeta(k)) \geq \gamma], \tag{18}$$

where $\gamma = |1 + W(w_u)|$ and γ follows a Rician distribution $p_0(\gamma)$ with Rician factor $\kappa = 1/2\sigma^2$. Then the SER of uncoded LoRa communication can be further written as

$$\begin{aligned} P_e &= 1 - \int_0^{\infty} [(\int_0^{\gamma} p_{\mathrm{n}}(\zeta)\,\mathrm{d}\zeta)^{2^{SF}-1} \cdot p_0(\gamma)]\,\mathrm{d}\gamma \\ &= \sum_{i=1}^{M-1} \frac{(-1)^{i-1}}{i+1} \binom{M-1}{i} \exp(-\frac{i}{2(i+1)\sigma^2}), \end{aligned} \tag{19}$$

Since LoRa adopts a relatively high order modulation which reaches $M = 4096$ when $SF = 12$, the combination term in (19) would suffer from precision problems during the evaluation of P_e. According to the deduction in [13], a more concise approximation for P_e becomes

$$P_e \approx Q(\sqrt{\frac{1}{\sigma^2}} - \sqrt{1.386SF + 1.154}). \tag{20}$$

Based on the above analysis, we analyze the BER performance of uncoded TDM-LoRa modulation. When multiplying $r(n)$ by $s_d(n)$, according to (9) and (12), the energy of $g_{u,d}(n)$ is concentrated at w_u^{th} frequency bin index. Since $g_{d,d}(n)$ is a sweep-frequency signal, its effect on each frequency bin index can be regarded as the same. With the increase of SF, $g_{d,d}(n)$ has much less influence on the w_u frequency bin index than $g_{u,d}(n)$ and can be ignored. Therefore we can approximate

$$\begin{aligned} G_d(k) &= |DFT[r(n)s_d(n)]| \\ &= |\sqrt{\frac{1}{2}}G_{u,d}(k) + \sqrt{\frac{1}{2}}G_{d,d}(k) + W(k)| \\ &\approx \begin{cases} |\sqrt{\frac{1}{2}} + W(w_u)| & k = w_u \\ |\sqrt{\frac{1}{2M}} + W(k)| & k \neq w_u, \end{cases} \end{aligned} \tag{21}$$

Consequently, the error rate of uncoded TDM-LoRa up-chirp component can be approximated by

$$\begin{aligned} P_{e0} &\approx \sum_{i=1}^{M-1} \frac{(-1)^{i-1}}{i+1} \binom{M-1}{i} \exp(-\frac{(\sqrt{\frac{1}{2}} - \sqrt{\frac{1}{2M}})^2 i}{2(i+1)\sigma^2}) \\ &\approx Q(\sqrt{(\sqrt{\frac{1}{2}} - \sqrt{\frac{1}{2M}})^2 \cdot \frac{2}{\sigma^2}} - \sqrt{1.386SF + 1.154}), \end{aligned} \tag{22}$$

As deduced in [12], if a symbol with the given SF is received in error, then for any given bit position of the binary representation, there are 2^{SF-1} of all possible $2^{SF} - 1$ ways that the chosen bit can be in error (one of the 2^{SF} possibilities is correct). Since the error rate of down-chirp component is also equal to P_{e0}, the BER of uncoded TDM-LoRa can be estimated as

$$P_{eb} = \frac{2^{SF-1}P_{e0}}{2^{SF} - 1}. \tag{23}$$

III. In-Phase and Quadrature Time Domain Multiplexed LoRa

To further improve the SE of our scheme, we propose an IQTDM-LoRa modulation based on IQCSS [8].

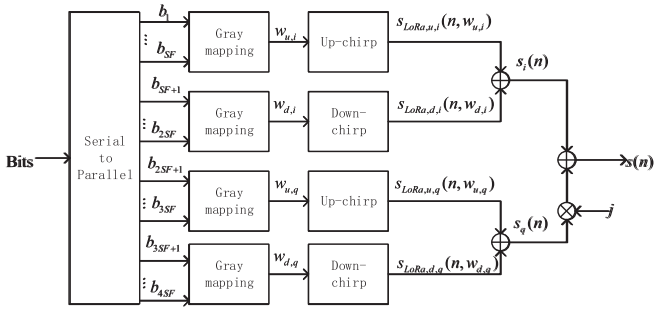

Fig. 4. Transmitter of the IQTDM-LoRa scheme.

According to [8], the information carried by LoRa symbols mainly lies in the real part of $R_{LoRa}(k)$. Therefore, if the phase rotation induced by the channel is corrected, the transmitted data symbol can be estimated as

$$\hat{w}_u = \arg\max_{0\le k<M} \Re(G_{u,d}(k)). \tag{24}$$

Accordingly, we propose the IQTDM-LoRa scheme. As shown in Fig. 4, we encodes information bits on both in-phase and quadrature components of the TDM-LoRa symbol. The discrete time IQTDM-LoRa symbol is given by

$$s_{i,q}(n) = (s_i(n) + js_q(n))/\sqrt{2}, \tag{25}$$

where

$$s_i(n) = (s_{LoRa,u,i}(n, w_{u,i}) + s_{LoRa,d,i}(n, w_{d,i}))/\sqrt{2}, \tag{26}$$

and

$$s_q(n) = (s_{LoRa,u,q}(n, w_{u,q}) + s_{LoRa,d,q}(n, w_{d,q}))/\sqrt{2}, \tag{27}$$

are our proposed TDM-LoRa symbols, and $w_{u,i}$, $w_{d,i}$, $w_{u,q}$ and $w_{d,q}$ are mappings of 4 groups of SF bits, respectively. Therefore, the IQTDM-LoRa scheme can double the data rate and SE of TDM-LoRa, and its SE can be written as

$$(4SF/T)/B = 4SF/(B \cdot T) = 4SF/2^{SF}. \tag{28}$$

Fig. 5 shows the coherent demodulation process of IQTDM-LoRa. The received symbol $r_{i,q}(n) = s_{i,q}(n) + w(n)$ is multiplied by $s_d(n)$ and $s_u(n)$, respectively. After DFT operation, we can get the estimated data symbol from the real and imaginary part frequency bin index with the peak value. And the estimated data symbols are

$$\begin{aligned}
\hat{w}_{u,i} &= \arg\max \Re[DFT(r_{i,q}(n)s_d(n))], \\
\hat{w}_{u,q} &= \arg\max \Im[DFT(r_{i,q}(n)s_d(n))], \\
\hat{w}_{d,i} &= \arg\max \Re[DFT(r_{i,q}(n)s_u(n))], \\
\hat{w}_{d,q} &= \arg\max \Im[DFT(r_{i,q}(n)s_u(n))].
\end{aligned} \tag{29}$$

Then the information bits can be obtained. It is worth noting that channel compensation is required for compensating the channel induced phase rotation on the transmit signal since both of IQCSS and IQTDM-LoRa schemes need employ coherent demodulation. Therefore, both schemes require a higher complexity receiver than TDM-LoRa.

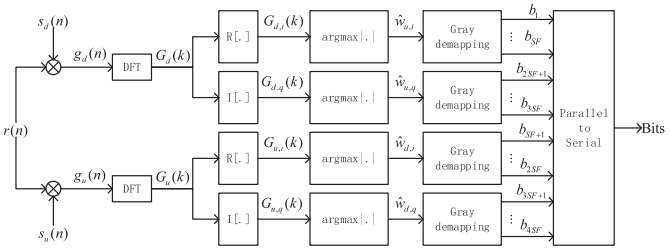

Fig. 5. Receiver of the IQTDM-LoRa scheme.

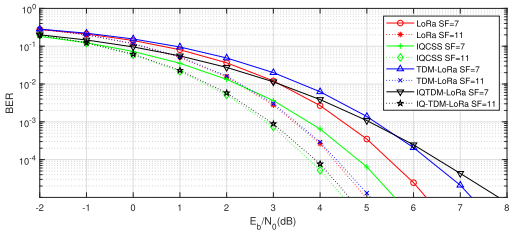

Fig. 6. BER performance under AWGN channels.

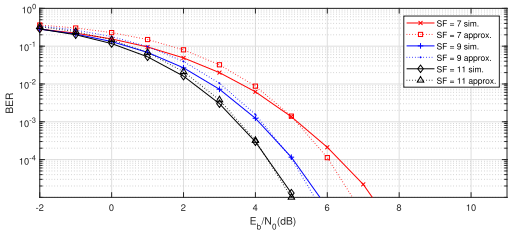

Fig. 7. BER performance of TDM-LoRa under AWGN channels.

IV. Simulations and Numerical Results

In the following, we compare the performance of the proposed TDM-LoRa modulation scheme with that of conventional LoRa, IQCSS and improved IQTDM-LoRa modulation in AWGN and Rayleigh fading channels.

Fig. 6 plots the BER versus E_b/N_0 of these schemes of different SFs under AWGN channels when $B = 125kHz$, Here, E_b/N_0 is the signal-to-noise ratio (SNR) per bit. It can be seen that larger SF will result in better performance. Since LoRa modulation adopts a kind of multiple Frequency Shift Keying (FSK), adding more symbols to the constellation does not reduce the minimum symbol distance. There is less than 1dB gap between LoRa and TDM-LoRa. As SF becomes larger, the BER performance gap between our proposed scheme and the conventional LoRa will decrease, due to the reduction of interference. With the increase of SF, the BER performance of IQTDM-LoRa improves faster than TDM-LoRa.

The derived approximations of uncoded TDM-LoRa (dotted curves) in (23) are plotted against simulation results (solid curves) in Fig. 7. It can be seen that the concise formula in (23) provides a small approximation gap within 0.4dB. With the increase of SF, the interference between up and down components will be reduced. Therefore as the figure shows, the accuracy of approximation is also improved.

Fig. 8 shows the BER under Rayleigh fading channels for these schemes. It can be observed that the BER performance difference among the four schemes is small and Rayleigh fading imposes severe impact on the BER performance.

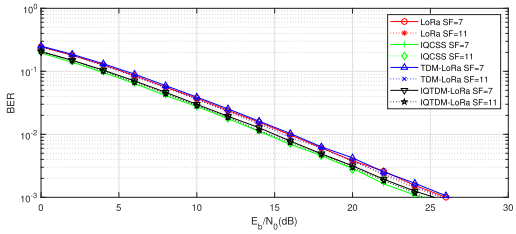

Fig. 8. BER performance under Rayleigh fading channels.

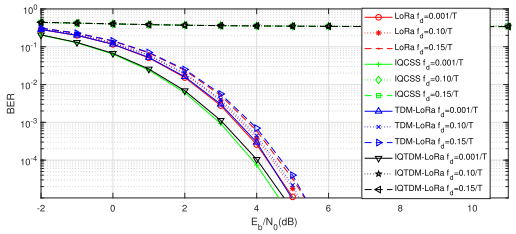

Fig. 9. BER performance under AWGN with different normalized carrier frequency offsets.

Fig. 9 depicts the BER performance of these schemes ($SF = 11$) in AWGN channels with different normalized carrier frequency offsets, respectively. There are 40 symbols in one frame. It can be seen that our proposed TDM-LoRa is as resilient to frequency offsets as the typical LoRa. However, both IQCSS and IQTDM-LoRa schemes can only work under better synchronization conditions. Our proposed IQTDM-LoRa can be applied to scenarios with better synchronization conditions that require higher data rates.

According to [8], the theoretical throughput of LoRa is

$$R = (1 - BER)SF/T = (1 - BER) \cdot B \cdot SF/2^{SF}, \quad (30)$$

that of TDM-LoRa and IQCSS is

$$R = (1 - BER) \cdot 2SF/T = (1 - BER) \cdot B \cdot SF/2^{SF-1}, \quad (31)$$

as for IQTDM-LoRa is

$$R = (1 - BER) \cdot 4SF/T = (1 - BER) \cdot B \cdot SF/2^{SF-2}. \quad (32)$$

Since the BER curves are very close to each other for all schemes in case of perfect synchronization. It can be obtained that TDM-LoRa achieves nearly 2 times throughput of LoRa, and IQTDM-LoRa further increases the throughput by nearly 2 times than TDM-LoRa. Our improved methods make more efficient usage of spectrum resources and satisfy the requirements for more IoT application.

V. Conclusion

Inspired by the LoRa PHY for wireless applications that require low energy consumption and larger data throughput, we propose TDM-LoRa modulation and IQTDM-LoRa modulation. We also obtain an analytical expression for the BER of TDM-LoRa modulation in AWGN channel. Simulation results show that the TDM-LoRa can double the data rate of LoRa without significant BER performance deterioration. Additionally, the proposed TDM-LoRa is as resilient to time and frequency offsets as the typical LoRa.

References

[1] C. Goursaud and J. M. Gorce, "Dedicated networks for IoT: PHY/MAC state of the art and challenges," *EAI Endorsed Trans. Internet Things*, vol. 1, no. 1, Oct. 2015, Art. no. 150597.

[2] M. Centenaro, L. Vangelista, A. Zanella, and M. Zorzi, "Long-range communications in unlicensed bands: The rising stars in the IoT and smart city scenarios," *IEEE Wireless Commun.*, vol. 23, no. 5, pp. 60–67, Oct. 2016.

[3] L. Vangelista, "Frequency shift chirp modulation: The LoRa modulation," *IEEE Signal Process. Lett.*, vol. 24, no. 12, pp. 1818–1821, Dec. 2017.

[4] T. T. Nguyen, H. H. Nguyen, R. Barton, and P. Grossetete, "Efficient design of chirp spread spectrum modulation for low-power wide-area networks," *IEEE Internet Things J.*, vol. 6, no. 6, pp. 9503–9515, Dec. 2019.

[5] R. Bomfin, M. Chafii, and G. Fettweis, "A novel modulation for IoT: PSK-LoRa," in *Proc. IEEE 89th Veh. Technol. Conf. (VTC-Spring)*, Apr. 2019, pp. 1–5.

[6] P. Edward, S. Elzeiny, M. Ashour, and T. Elshabrawy, "On the coexistence of LoRa- and interleaved chirp spreading LoRa-based modulations," in *Proc. Int. Conf. Wireless Mobile Comput., Netw. Commun. (WiMob)*, Oct. 2019, pp. 1–6.

[7] M. Hanif and H. H. Nguyen, "Slope-shift keying LoRa-based modulation," *IEEE Internet Things J.*, vol. 8, no. 1, pp. 211–221, Jan. 2021.

[8] I. B. F. de Almeida, M. Chafii, A. Nimr, and G. Fettweis, "In-phase and quadrature chirp spread spectrum for IoT communications," in *Proc. GLOBECOM IEEE Global Commun. Conf.*, Dec. 2020, pp. 1–6.

[9] X. Wang, M. Fei, and X. Li, "Performance of chirp spread spectrum in wireless communication systems," in *Proc. 11th IEEE Singap. Int. Conf. Commun. Syst.*, Nov. 2008, pp. 466–469.

[10] H. Wang and A. O. Fapojuwo, "A survey of enabling technologies of low power and long range machine-to-machine communications," *IEEE Commun. Surveys Tuts.*, vol. 19, no. 4, pp. 2621–2639, Jan. 2017.

[11] G. Baruffa, L. Rugini, L. Germani, and F. Frescura, "Error probability performance of chirp modulation in uncoded and coded LoRa systems," *Digit. Signal Process.*, vol. 106, Nov. 2020, Art. no. 102828.

[12] M. K. Simon and M.-S. Alouini, *Digital Communication Over Fading Channels*, 2nd ed. Hoboken, NJ, USA: Wiley, 2005.

[13] T. Elshabrawy and J. Robert, "Closed-form approximation of LoRa modulation BER performance," *IEEE Commun. Lett.*, vol. 22, no. 9, pp. 1778–1781, Sep. 2018.